The 2009 IEEE/RSJ International Conference on
Intelligent Robots and Systems
October 11-15, 2009 St. Louis, USA

SURALP: A New Full-Body Humanoid Robot Platform

Kemalettin Erbatur, *Member, IEEE,* Utku Seven, Evrim Taşkıran, Özer Koca, Metin Yılmaz, Mustafa Ünel, *Member, IEEE,* Güllü Kızıltaş, Asif Sabanovic, *Senior Member, IEEE* and Ahmet Onat, *Member, IEEE*

Abstract— **SURALP is a new walking humanoid robot platform designed at Sabanci University - Turkey. The kinematic arrangement of the robot consists of 29 independently driven axes, including legs, arms, waist and a neck. This paper presents the highlights of the design of this robot and experimental walking results. Mechanical design, actuation mechanisms, sensors, the control hardware and algorithms are introduced. The actuation is based on DC motors, belt and pulley systems and Harmonic Drive reduction gears. The sensory equipment consists of joint encoders, force/torque sensors, inertial measurement systems and cameras. The control hardware is based on a dSpace digital signal processor. A smooth walking trajectory is generated. A variety of controllers for landing impact reduction, body inclination and Zero Moment Point (ZMP) regulation, early landing trajectory modification, and foot–ground orientation compliance and independent joint position controllers are employed. A posture zeroing procedure is followed after manual zeroing of the robot joints. The experimental results indicate that the control algorithms presented are successful in improving the stability of the walk.**

I. Introduction

THE bipedal kinematic arrangement is suitable for the human environment. It can avoid typical obstacles and operate systems in this environment like human do. This is one of the important motivations for the intensive research focused on humanoid robotics in the last four decades. Many successful projects and results are reported [1-5].

One of the most challenging problems in this field is the robust balance of the walk. A number of complications are caused by the nonlinear and hard-to-stabilize dynamics of the free-fall robot and the coupling effects between the many degrees of freedom [6]. The difficulties are even more pronounced in unstructured environments such as on uneven floor [7, 8].

Manuscript received March 1, 2009. This work was supported by The Scientific and Technological Research Council of Turkey under Project Grant No. 106E040.

The authors are with the Faculty of Engineering and Natural Sciences, Sabancı University, Istanbul, 34956 Turkey (phone: +90-216-483-9585; fax: +90-216-483-9550; e-mail: erbatur@sabanciuniv.edu, utkuseven@su.sabanciuniv.edu, evrimt@su.sabanciuniv.edu, ozerk@su.sabanciuniv.edu, metinyilmaz@su.sabanciuniv.edu, munel@sabanciuniv.edu, gkiziltas@sabanciuniv.edu, asif@sabanciuniv.edu, onat@sabanciuniv.edu).

In 2006, Sabanci University - Turkey initiated experimental research on bipedal walking in the framework of a project funded by TUBITAK (The Scientific and Technological Research Council of Turkey). The main research targets are bipedal walking on uneven surfaces and manipulation by virtue of visually-aided force control. A human sized full body humanoid robot, SURALP (Sabanci University Robotics ReseArch Laboratory Platform) is designed as the test platform in this project. SURALP is a robot with 29 DOFs, including leg, arm, neck and waist joints. 12 DOF leg module was introduced in [9, 10]. This paper introduces the full body robot SURALP from the mechanical design, sensor feedback and control system aspects. Experimental walking results are presented too.

The actuation mechanisms of the robot are constructed with DC motors, belt and pulley systems and Harmonic Drive reduction gears. Inertial measurement systems, force/torque sensors, joint incremental encoders and CCD cameras are used for sensory feedback. The control and data acquisition hardware is based on a dSpace digital signal processor board. A smooth walking trajectory is generated. Independent joint PID position controllers are employed to track joint references. Mismatches between the planned and actual walking are compensated by a number of additional controllers, which exploit sensory feedback. These additional controllers include a ground impact compensator, an early landing gait modification system, a ZMP control and algorithms for foot and trunk orientation correction. Also, zeroing a biped robot is critical and an automatic zeroing algorithm is applied in this study.

The paper is organized as follows. Section II introduces the kinematic arrangement, limits and dimensions of the mechanical system with information on actuation and transmission systems. The mechanical design and analysis methods are briefed in Section II too. Sensor systems are detailed in Section III. Section IV outlines the controller hardware. The employed control laws are presented in Section V. Experimental walking results are discussed in Section VI. In Section VII, the conclusion and a discussion on future work are presented.

II. Mechanical Design and Actuators

The biped robot SURALP with control hardware in its trunk is shown in Fig. 1 and 2. It is designed in human proportions. Hips are composed of three orthogonal joint axes intersecting each other at a common point.

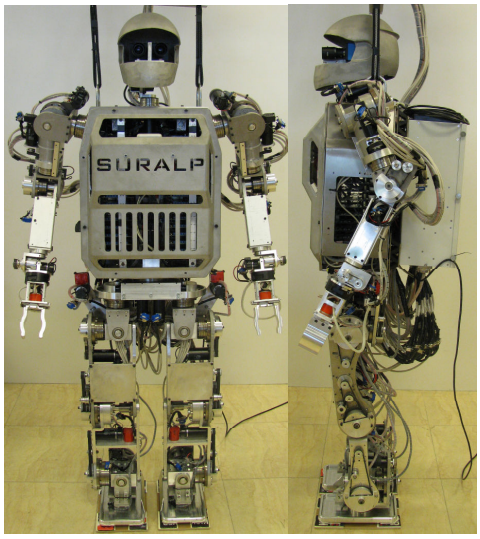

Fig. 1 SURALP, side and front views.

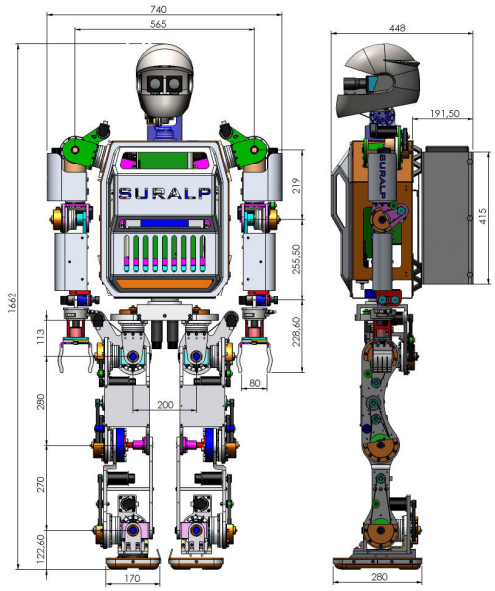

Fig. 2 SURALP, dimensions.

In the kinematic arrangement, the knee axis follows the hip pitch axis. The ankle accommodates two orthogonal axes: ankle pitch and ankle roll. There is a waist yaw axis positioned on the pelvis. The axes of the 6-DOF arms are as follows: The shoulder motion is realized by three orthogonal joint axes. These axes are followed by a revolute elbow joint. A roll and a pitch axis positioned in the forearm actuate the wrist. The single DOF hand opens and closes linearly. The neck is composed of joint arranged in the pan-tilt configuration (Fig. 3). The link length and weight information is tabulated in Table I.

After the preliminary mechanical design, simulation studies are carried out in a Newton-Euler method based full-dynamics 3D simulation and animation environment as described in [11]. The force and torque vectors acting on the two ends of robot links are computed and recorded during the simulated walk with the reference trajectories in [11].

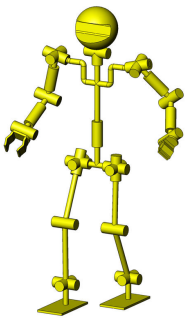

Fig. 3 The kinematic arrangement of. SURALP.

TABLE I
LENGTH AND WEIGHT PARAMETERS

Upper Leg Length	280mm
Lower Leg Length	270mm
Sole-Ankle Distance	124mm
Foot Dimensions	240mm x 150mm
Upper Arm Length	219mm
Lower Arm Length	255mm
Robot Weight	101 kg

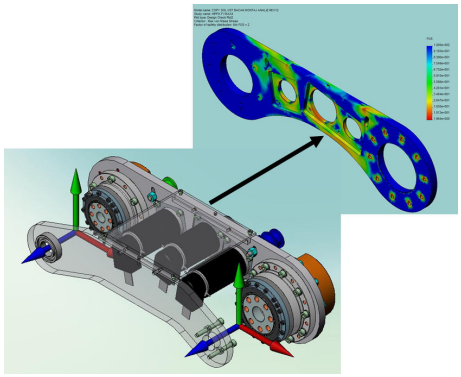

Fig. 4 Finite element analysis window for the upper leg main lame

Fig. 4 shows the CAD model of the upper leg with two coordinate frames attached to each link end. The link end force and torque vectors recorded in the simulations are expressed in these coordinate frames. Finite element analysis is then carried out with a solid modeling software tool, using the recorded force and torque values as inputs. In this way, the strength of each link is computed and the thickness of the lames used in the design is determined. Aircraft aluminum is chosen as the construction material. Fig. 4 also shows a window from the solid modeling and analysis package, for the main lame of the upper leg which is expected to be the most deformed component. Also obtained from the Newton-Euler based simulation are the torque capacity and velocity range requirements of the DC motors and reduction gears used at the motor joints. Belt-pulley systems transmit the motor rotary motion to Harmonic Drive reduction gears. In this way, very high reduction ratios can be obtained in a very compact space. All joints, except the knee joint are actuated by a single DC motor. The knee joint is driven by two DC motors for high torque capability. Table II displays the motor powers, belt-pulley and the Harmonic Drive reduction ratios. Also shown in this table are the working ranges of the joints.

TABLE II
JOINT ACTUATION SYSTEMS

Joint	Motor Power	Pulley Ratio	HD Ratio	Motor Range
Hip-Yaw	90W	3	120	-50 to 90 deg
Hip-Roll	150W	3	160	-31 to 23 deg
Hip-Pitch	150W	3	120	-128 to 43 deg
Knee 1	150W	3	160	-97 to 135 deg
Knee 2	150W			
Ankle-Pitch	150W	3	100	-115 to 23 deg
Ankle Roll	150W	3	120	-19 to 31 deg
Shoulder Roll 1	150W	2	160	-180 to 180 deg
Shoulder Pitch	150W	2	160	-23 to 135 deg
Shoulder Roll 2	90W	2	120	-180 to 180 deg
Elbow	150W	2	120	-49 to 110 deg
Wrist Roll	70W	1	74	-180 to 180 deg
Wrist Pitch	90W	1	100	-16 to 90 deg
Gripper	4W	1	689	0 to 80 mm
Neck Pan	90W	1	100	-180 to 180 deg
Neck Tilt	70W	2	100	-24 to 30 deg
Waist	150W	2	160	-40 to 40 deg

TABLE III

SENSORS OF SURALP

	Sensor	Number of Channels	Range
All joints	Incremental optic encoders	1 channel per joint	500 pulses/rev
Ankle	F/T sensor	6 channels per ankle	± 660 N (x, y-axes) ± 1980 N (z-axis) ± 60 Nm (all axes)
Foot	FSR	4 channels per foot	0 to 250 N
Torso	Accelerometer	3 channels	± 2 G
	Inclinometer	2 channels	± 30 deg
	Rate gyro	3 channels	± 150 deg/s
Wrist	F/T sensor	6 channels per wrist	± 65 N (x, y-axes) ± 200 N (z-axis) ± 5 Nm (all axes)
Head	CCD camera	2 with motorized zoom	640x480 pixels 30 fps

III. SENSORY SYSTEMS

The sensory system of SURALP includes sensors in the following four categories: i) encoders measuring the motor angular positions, ii) force and torque sensors, iii) inertial sensors and iv) CCD cameras.

The motor positions are measured by 500 ppr optic incremental encoders.

6 axis force/torque sensor which is positioned at the ankle are used to obtain external force data. The ankle torques and the vertical direction total ground interaction force can be measured by this system.

The robot is equipped by a rate gyro, an inclinometer, and a linear accelerometer which are mounted at the robot torso too.

These sensors are listed in Table III with their working ranges and mounting locations.

IV. CONTROLLER HARDWARE

The control electronics is based on dSpace modular hardware. A DS1005 board of the dSpace family is central in our controller. This is the board where all the control algorithms explained in the next section run. Seven DS3001 incremental encoder input boards provide connectivity for 35 joint encoders. 31 of the connections provided by these boards are occupied with the encoders of the current design of SURALP. DS2002 and DS2103 boards are used for analog inputs and outputs, respectively.

The rate gyro, accelerometer, inclinometer, FSR sensors and 6-axis force/torque sensors are integrated over the analog inputs. The analog outputs provide torque references for the four-quadrant Maxon & Faulhaber DC motor drivers. The control and data acquisition boards mentioned above are housed by a dSpace Tandem AutoBox enclosure, which is mounted in a backpack configuration in the robot assembly. The power source and a remote user interface computer are placed externally. The CCD cameras are connected to the remote control PC via Firewire interfaces.

V. CONTROL ALGORITHM

The joint position references are generated through inverse kinematics from Cartesian foot references defined in world frame coordinates. Typical position references for the feet are shown in Fig. 5. The foot orientation references used in inverse kinematics are fixed and they are computed for feet parallel to the ground and robot body oriented with a small pitch angle (4 degrees) with respect to the ground. By virtue of the body pitch angle, the robot center of mass, which is behind the waist axis, is moved forward, closer to the center of the pelvis. The waist axis reference is in the form of the left leg x-direction reference shown in Fig. 5. It has however amplitude of 6 degrees. The waist motion is used to counteract the angular momentum created by the swinging leg.

Independent joint PID controllers are employed and the controller gains are obtained via trial and error. We propose the following additional control techniques to achieve stable walking.

Foot orientation control:

In [3] landing orientation controllers are proposed for the ankle joints. This approach assumes that two joints with coinciding joint axes perpendicular to each other are present at ankles. The scheme computes joint angle reference modifications in such a way that the feet are aligned parallel to the ground when they are in contact with the ground.

The reference modification law in [3] is the form of a first order filter applied on the foot to ground contact torques. We adopted this method for our control system too. For the roll axis of the ankle, we employ the following reference modification law in the Laplace domain.

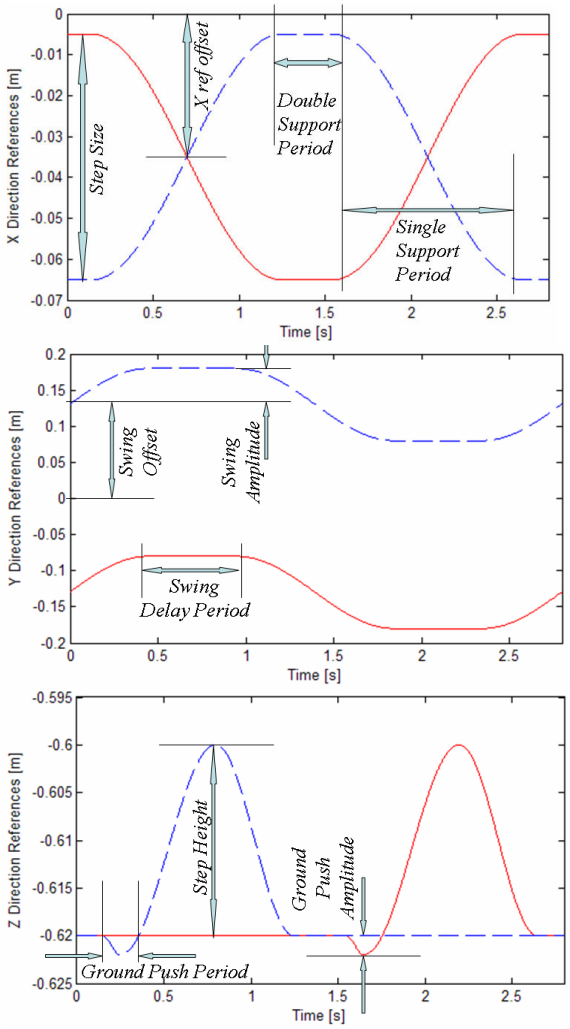

Fig. 5 Cartesian reference trajectories for the feet as expressed in a coordinate frame attached to the trunk. (Solid curves represent references for the right leg, dashed ones are for the left leg.)

$$\bar{\theta}_{roll}(s) = \theta_{roll}(s) + \frac{K_{roll}}{s + \lambda_{roll}} T_{roll}(s) \qquad (1)$$

where s is the Laplace variable. θ_{roll} is the roll joint reference angle computed from the inverse kinematics with CoM reference input. $\bar{\theta}_{roll}$ is the reference angle after the reference modification. T_{roll} is the torque about the roll axis due to the interaction of the foot with the ground. T_{roll} is measured by torque sensors positioned at the ankle. K_{roll} and λ_{roll} are low pass filter constants which are determined by trial and error in our approach. In the digital implementation, the Laplace domain transfer function in (1) is approximated by a difference equation. We used Tustin's approximation technique to obtain the difference equation.

When the foot is in contact with the ground only with a corner or an edge, a torque is developed and with the application of (1), the joint angle references are modified in such a way to turn the ankle to achieve foot orientation parallel to the ground.

Ground impact compensation:

Another important problem in achieving stable walking is the impact generated at the landing of the swing foot. As a solution, [4] suggests the application of a shock absorber control law. This control law is activated when the swing foot lands earlier than planned in the reference generation. In effect, a virtual mass-spring-damper system is positioned between the hip and ankle. Inspired by this idea, we employed the following second order relation to modify the distance between the hip and sole of the landing foot.

$$\bar{l}(s) = l(s) - \frac{1}{m_l s^2 + b_l s + k_l} F_z(s) \qquad (2)$$

In (2) l represents the hip-to-sole distance reference obtained from Cartesian foot reference trajectories. $\bar{l}$ is its shock absorber modified version. F_z is the z direction component of the ground interaction force acting on the foot. Again, ankle or sole-mount force sensors measure this force. m_l, b_l and k_l are the desired mass, damping and stiffness parameters of the mechanical impedance relation described in (2). Our impact compensator is triggered with any landing (not just for the early landing) of the foot. It is deactivated after a certain time specified by the control designer. In our case we used a 0.4 seconds activation time. However, at the end of this activation time the hip-to-sole distance is no more equal to its original value. In order to resume the hip-to-sole distance which is originally planned in the reference generation process, at the end of the impact compensation phase the following relation is employed:

$$\bar{l}(t) = l(t) - 0.5(l(t_0) - \bar{l}(t_0))\left(1 + \cos((t_0 - t)\omega_{return}\right). \qquad (3)$$

t_0 is the time at the end of the impact compensation phase. By (3), beginning with the final $\bar{l}$ value of the impact compensation phase, $\bar{l}$ returns to the original reference value l after a smooth transient behaviour. ω_{return} is a parameter which determines the speed of return of $\bar{l}$ to l. As in the case of (1), Tustin's approximation of the continuous relation is obtained and applied for (2) and (3) too.

The reference modification laws, (1), (2) and (3) are applied to the two legs independently.

Early landing modification:

One of the main problems of early landing of a swung foot is that when it is on the ground before the planned beginning of the double support phase, it will go on moving forward. When we inspect the x direction foot references shown in Fig. 5, we will see that the other foot (the planned support foot) will move at the same time backward in a trunk based coordinate system. In effect, the two feet on the ground will try to push the robot trunk in two different directions. The feet will slip, the robot will turn and possibly loose it balance. In order to avoid such a condition, the x direction references in Fig. 5 are modified in the case of an early landing. Specifically, this modification "stops" the x direction references of the feet at their values they had at the

instant of early landing. These references are kept fixed until the next walking cycle and start from their fixed values, whenever the planned x direction references reach them again.

Trunk orientation control:

The inclination of the robot body (or trunk) is an important indicator of the stability of the walk. Also, in many applications, a vertical trunk is desirable. In order to keep the trunk vertically aligned on uneven ground conditions [4] proposes the simultaneous control of effective leg lengths and ankle pitch/roll angles. In our experimental work, we followed the same route as in [4]. In the sagittal direction part of this controller the ankle pitch angles are modified by using feedback from body inclination. We used inclinometer data in this controller. The control law employed is

$$\bar{\theta}_{pitch}(s) = \theta_{pitch}(s) + \left(K_{P-pitch} + K_{I-pitch}\frac{1}{s} \right)\theta_{trunk\ pitch}(s) \qquad (4)$$

where $\theta_{pitch}(s)$ is the pre-planned pitch angle reference for the ankle joints (for the right ankle and the left ankle) and $\bar{\theta}_{pitch}(s)$ is the modified reference. $\theta_{trunk\ pitch}(s)$ is the trunk pitch angle measured by the inclinometer. $K_{P-pitch}$ and $K_{I-pitch}$ are the trunk pitch control proportional and integral action gains, respectively. In the lateral direction, for the ankle roll joints, the landing foot orientation controller described above in this section is employed. The trunk roll angle control is carried out by using the effective leg lengths which in our study are defined as the distances between the hip joints and foot soles. The feedback law which uses the inclinometer roll angle measurement is as follows.

$$\begin{aligned} \bar{l}_{left}(s) &= l_{left}(s) + \left(K_{P-roll} + K_{I-roll}\frac{1}{s} \right)\theta_{trunk\ roll}(s) \\ \bar{l}_{right}(s) &= l_{right}(s) - \left(K_{P-roll} + K_{I-roll}\frac{1}{s} \right)\theta_{trunk\ roll}(s) \end{aligned} \qquad (5)$$

In these expressions, l_{left} and l_{right} are the pre-planned effective lengths of the left and right leg, respectively. $\bar{l}_{left}$ and $\bar{l}_{right}$ are their versions after the application of the trunk orientation controller. K_{P-roll}, K_{I-roll}, K_{P-roll} and K_{I-roll} are controller gains and $\theta_{trunk\ roll}$ is the measured trunk roll angle. (5) and the impact compensator defined by (2) and (3) are applied to the effective leg joints with superposition.

ZMP regulation:

The ZMP criterion is widely used as a measure of stability of the bipedal walk. The ZMP should be inside the supporting polygon of the two feet in the double support phase and inside the supporting sole area in the single support phases. In this paper, we employed ZMP control for the homing (zeroing) process of the robot. For this purpose, a simple proportional action relation between the ZMP error and pelvis horizontal position proved to be successful. The ZMP reference for zeroing the robot is defined in the middle of the supporting polygon as in Fig. 8.

$$\begin{aligned} &\bar{X}_{ref\ offset}(s) = \\ &X_{ref\ offset}(s) + K_{P-ZMP\ X}\left(X_{ZMP\ desired}(s) - X_{ZMP\ actual}(s)\right) \end{aligned} \qquad (6)$$

$$\begin{aligned} &\bar{Y}_{ref\ offset}(s) = \\ &Y_{ref\ offset}(s) + K_{P-ZMP\ Y}\left(Y_{ZMP\ desired}(s) - Y_{ZMP\ actual}(s)\right) \end{aligned} \qquad (7)$$

$X_{ref\ offset}$ and $Y_{ref\ offset}$ are the center locations of the Cartesian reference trajectories shown in Fig.4. $\bar{X}_{ref\ offset}$ and $\bar{Y}_{ref\ offset}$ are their modified versions.

Fig. 9 shows the control methods and the sensors used for them in a block diagram. These controllers are not all used simultaneously. For homing purpose, foot pitch torque difference compensation, ZMP regulation and foot and trunk orientation controllers are employed whereas during the walk foot orientation control, ground impact compensation, early landing modification, foot pitch torque difference compensation and foot and trunk orientation controllers are used. Also it should be mentioned that the trunk orientation controller for walking purposes is tuned with larger proportional and integral gain constants when compared with the trunk orientation control for the homing purpose. This choice is made in order to obtain a faster response in walking. Experimental results with controllers described in this section are presented in Section VI.

VI. Experimental Results

The controllers discussed in Section V are employed for walking experiments with SURALP. Table IV shows trajectory generation parameters corresponding to the foot Cartesian references in Fig. 5. The various control parameters of Section V and the reference generation parameters in Table IV are obtained by trial and error.

The comparison of the original and the modified ankle roll angle references shows the effect of the foot orientation control. Ankle pitch angle references are modified in a way similar shown in this figure too. The foot orientation control modifies the ankle joint references to keep the feet parallel to the ground.

The modification of the hip-to-sole distance of the right leg by the ground impact compensation is shown in Fig. 7. As explained in Section V, using the measured ground interaction force on the landing foot, the impact is absorbed via a second order virtual mass-spring-damper system. After the activation time defined by the control designer, the modified distance returns to its original value by a smooth transition, as given in equation (4). The stability of the walk is verified by the smoothness and the repeatability of the modification of the hip-to-sole distance.

TABLE IV
TRAJECTORY GENERATION PARAMETERS

Single sup. period	1.2 s
Double sup. period	1.2 s
Ground push period	0.8 s
Swing delay period	0.5 s
Step period	4.8 s
Step height	5mm
Body pitch angle	4 deg
Step size	5 cm
Ground push amp.	1 cm
Swing amplitude	6 cm
Swing offset	14 cm
Body height	62 cm
Initial *x*-ref offset	-6.5cm
Waist motion amp.	6 deg

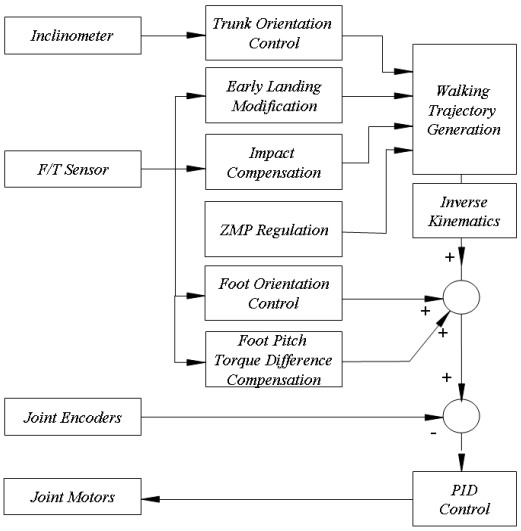

Fig. 6 The control block diagram.

The trunk roll and pitch angle oscillations during the walk are measured by the inclinometer located on the trunk of the robot and shown in Fig. 8. They indicate the steady nature of the walk obtained by the use of the control system too.

VII. CONCLUSION

A new full-body humanoid robotics experimental platform, SURALP, is introduced in this paper. Mechanical design guidelines, actuators, sensors and control hardware are detailed. A smooth walking reference generation method and force/inertial feedback based controllers for SURALP are introduced. Experimental results indicate that the integrated robot system is suitable as a test bed for humanoid robotics. The controllers are successful in obtaining a steady walk. Our future work will be concentrated on visually assisted force control with the robot arms for environmental interaction and on improving the walking performance.

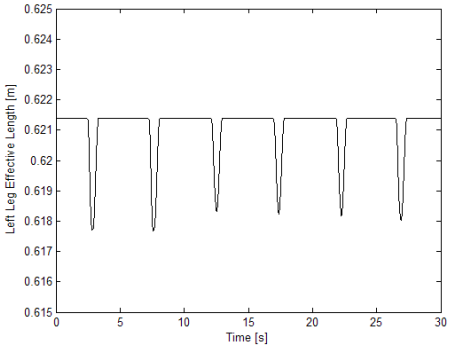

Fig. 7 Hip-to-sole distance modifications of the right leg.

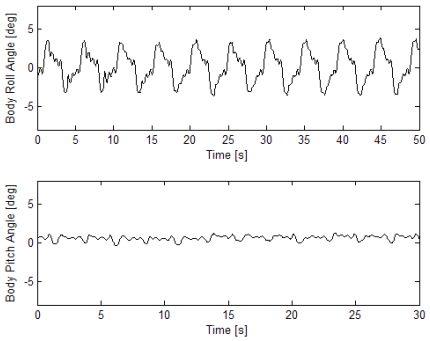

Fig. 8 Roll and pitch angle oscillations of the robot body

REFERENCES

[1] Y. Sakagami, R. Watanabe, C. Aoyama, M. Shinichi, N. Higaki, and K. Fujimura, "The intelligent ASIMO: System overview and integration", *Proceedings of the IEEE International Conference on Intelligent Robots and Systems*, Lausanne, Switzerland, October 2002

[2] K. Kaneko, F. Kanehiro, S. Kajita, K. Yokoyama, K. Akachi, T. Kawasaki, S. Ota, and T. Isozumi, "Design of prototype humanoid robotics platform for HRP", *IEEE International Conference on Intelligent Robots and Systems, pp.2431-2436, vol.3*, October 2002.

[3] Kim, J-H. and Oh J-H., "Realization of Dynamic Walking for the Humanoid Robot Platform KHR-1," *Advanced Robotics*, Vol. 18, No. 7, pp. 749–768 (2004)

[4] J. Y. Kim, I. W. Park, J. H. Oh, "Walking Control Algorithm of Biped Humanoid Robot on Uneven and Inclined Floor", *J Intell Robot Syst (2007) 48:457–484,* January 2007.

[5] Y. Ogura, H. Aikawa, K. Shimomura, H. Kondo, A. Morishima, H. Lim and A. Takanishi, "Development of A Humanoid Robot WABIAN-2," Proc. 2006 IEEE Int. Conference on Robotics and Automation, pp. 76-81, 2006

[6] M. Vukobratovic, B. Borovac, D. Surla and D. Stokic, *Biped Locomotion: Dynamics, Stability and App.*. Springer-Verlag, 1990.

[7] S. Kajita and K. Tani, "Adaptive Gait Control of a Biped Robot Based on Realtime Sensing of the Ground Profile," in *1996 Proc. IEEE Int. Conf. Robotics and Automation,* pp. 570-577.

[8] H. Hirukawa, S. Hattori, S. Kajita, K. Harada, K. Kaneko, F. Kanehiro, M. Morisawa and S. Nakaoka, "A Pattern Generator of Humanoid Robots Walking on a Rough Terrain," in *2007 Proc. IEEE Int. Conf. Robotics and Automation,* pp. 2181-2187.

[9] Erbatur, K., U. Seven, E. Taşkiran, Ö. Koca, G. Kızıltaş, M. Ünel, A. Sabanovic. A. Onat, "SURALP-L, The Leg Module of a New Humanoid Platform," *Proc. IEEE/RAS International Conference on Humanoid Robots*, Daejeon-Korea, December 2008

[10] Erbatur, K., U. Seven, E. Taşkiran, Ö. Koca "Walking Trajectory Generation and Force Feedback Control for The Humanoid Robot Leg Module Suralp-L" *Proc. IASTED International Conference on Intelligent Systems and Control*, Orlando USA, November 2008

[11] K. Erbatur and A. Kawamura, "A new penalty based contact modeling and dynamics simulation method as applied to biped walking robots," *Proc. 2003 FIRA World Congress*, October 1-3, 2003 Vienna, Austria